Estimation of minimum and maximum air temperature using MODIS data over Gujarat

D B SHAH[1,*], M R PANDYA[2], H J TRIVEDI[3], and A R JANI[1]

[1]*Department of Physics, Sardar Patel University, Vallabh Vidyanagar-388120*
[2]*Space Applications Centre, Indian Space Research Organization, Ahmedabad-380015*
[3]*N.V. Patel College of Pure and Applied Sciences, Vallabh Vidyanagar-388120*
Corresponding author: dhirajshah123@gmail.com

ABSTRACT

Minimum and maximum air temperatures are important input parameters for meteorological and agricultural models. Generally minimum and maximum air temperatures are measured at weather stations on the ground. However these measurements are not available with enough spatial density which makes it difficult to be used in real-time applications. Compensation of this lack of information can be achieved by satellite-based methods. The present study investigates the potential of deriving the spatial distribution of minimum and maximum air temperatures with the help of land surface temperature (Ts) and normalized differential vegetation index (NDVI) products from the moderate resolution imaging spectroradiometer (MODIS) sensor and air temperature (Ta) data from automatic weather stations (AWS) over Gujarat region of India. The minimum Ta was successfully retrieved through a regression analysis between night time MODIS Ts and AWS measured minimum Ta over all stations, since the minimum Ta is strongly associated with night time Ts. While, the maximum Ta was retrieved using a method, namely, temperature vegetation index (TVX) approach based on the linear relationship between Ts and NDVI data. Results showed that MODIS estimated minimum Ta were in good agreement with the measured values by mean absolute error (MAE) of 1.49 ^{0}C and root mean square error (RMSE) of 1.95 ^{0}C. While, maximum Ta retrieved through TVX approach showed a good retrieval accuracy with a MAE of 1.96 ^{0}C and RMSE of 2.46 ^{0}C.

Keywords: Land surface temperature, NDVI, air temperature, MODIS

Minimum and maximum air temperatures (hereafter called Ta_{min} and Ta_{max}) are important climatological variables and accurate mapping its spatial-temporal distribution is useful in wide range of applications in the field of ecology, hydrology and atmospheric sciences. Air temperature (Ta) has been traditionally measured at large number of meteorological stations. However such meteorological measurements are not usually available with enough spatial density for accurate research purposes (Vogt *et al.*, 1997; Willmott *et al.*, 1991). The spatio-temporal pattern of near surface Ta is complex because it is affected by properties that vary greatly in both space and time (Prihodko and Goward, 1997). Satellite-based remote sensing technique is an alternative to provide spatially distributed information, because of its capability of systematic and synoptic coverage over a large geographical area (Czajkowski *et al.*, 1997; Goward *et al.*, 1994). The satellite-derived Land Surface Temperature (Ts) has a significant relationship with the Ta in the boundary layer because of the process of conduction and convection of heat fluxes in the lower atmosphere, resulting from the radiative heating of the earth's surface (Oke, 1987). This effect will be prominent during clear sky days when land surface characteristics have a major influence on surface energy balance. Under such conditions, it should be possible to map the spatial pattern of the Ta with a higher accuracy, using remotely sensed observation. Satellite derived Ts and Normalized Differential Vegetation Index (NDVI) data provide an opportunity to estimate Ta_{min} and Ta_{max} (Nemani and Running, 1989; Goward *et al.*, 1994; Prihodko and Goward, 1997; Florio *et al.*, 2004). Earlier studies have focused basically on five approaches to estimate Ta_{min} and Ta_{max} namely; Statistical approach (Davis and Tarpley, 1983; Green and Hay, 2002; Florio *et al.*, 2004; Vancutsem *et al.*, 2010), empirical solar zenith angle approach (Cresswell *et al.*, 1999), energy balance approach (Sun *et al.*, 2005), TVX approach (Nemani and Running, 1989; Goward *et al.*, 1994 and
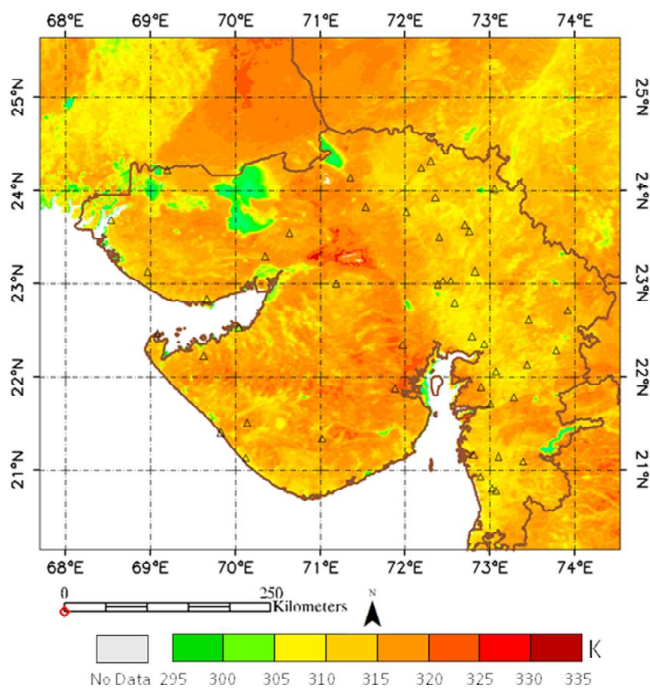
PAPER 2

Fig. 1: Location of ISRO-AWS network in Gujarat marked with '""' sign over a MODIS 8-day Ts image acquired on 14 March 2011

Prihodko and Goward, 1997) and Neural network approach (Jang *et al.*, 2004).

During the night time, the retrieval of Ta_{min} is simpler as solar radiation does not affect the thermal infrared signal and there exists a linear relationship between night time Ts and Ta_{min}. Here a simple statistical approach enables estimation of Ta_{min}. However, during day time estimation of Ta_{max} is not straight forward, since the difference between Ts and Ta_{max} is mainly controlled by the surface energy balance (Zaksek and Schroedter-Homscheidt, 2009), and many other parameters such as, incoming solar radiation, cloud-cover, wind speed, soil moisture and surface roughness affect the maximum Ta retrieval (Prince *et al.*, 1998). Earlier studies (Nemani and Running, 1989; Goward *et al.*,1994; Prihodko and Goward, 1997) have derived the Ta_{max} using satellite data using the correlation between Ts and NDVI measurements. Such approach of estimating Ta_{max} from the Ts-NDVI relationship is called the Temperature-Vegetation Index (TVX) approach. This method assumes that the temperature of a full cover canopy approaches the temperature of the air within the canopy (Czajkowski *et al.*, 1997; Prihodko and Goward, 1997).

The aim of this study was to estimate Ta_{min} and Ta_{max} over Gujarat for the year 2011 using satellite and ground

based observations. We first retrieve Ta_{min} using night time MODIS Ts data through linear regression analysis and then we use the TVX approach to retrieve Ta_{max} using MODIS Ts and NDVI data. Finally we validate the accuracy of the satellite-derived Ta_{min} and Ta_{max} using the AWS measured Ta_{min} and Ta_{max} observations.

MATERIALS AND METHODS

Study area

Gujarat state is located in the north-west of India between $20^0$1'N and $24^0$7'N latitude and $68^0$4'E and $74^0$4' E longitude (Fig. 1). This study area provides a natural variability in Ta (6-46 ^{0}C) due to its geographical regions and seasons. The state comprises three geographical regions: 1) a peninsula, traditionally known as Saurashtra, which is essentially a hilly tract sprinkled with low mountains; 2) Kutch on the north-east is barren and rocky and contains the famous Rann (desert) of Kutch, the big Rann in the north and the little Rann in the east; 3) the mainland extending from the Rann of Kutch and the Aravalli Hills to the river Damanganga is on the whole a level plain of alluvial soil. The climate of Gujarat is moist in the southern region and dry in the northern and western region. The year can be divided into: the winter season from November to February, the summer season from March to May, the monsoon season from June to September and intervening month of October.

Automatic weather station data

Air temperature data over Gujarat region was obtained from the network of 47 Automatic Weather Stations (AWS) established by the Indian Space Research Organization (ISRO). The hourly Ta data for the year 2011 was obtained from Meteorological and Oceanographic Satellite Data Archival Centre (MOSDAC site- http://www.mosdac.gov.in). The spatial distribution of the AWS stations over Gujarat is shown in Fig. 1. These hourly Ta data were converted to daily Ta_{min} and Ta_{max} observations and these daily observations were averaged to 8-day average Ta_{min} and Ta_{max} values.

MODIS data

The product of Ts is derived from two thermal infrared bands (31 and 32) of the MODIS sensor operating in 10.78–11.28 im and 11.77–12.27 im spectral regions through a split window algorithm (Wan and Dozier, 1996). In this study MODIS 8-day composite (MOD11A2 and MYD11A2) Ts data over Gujarat was used for the year 2011.
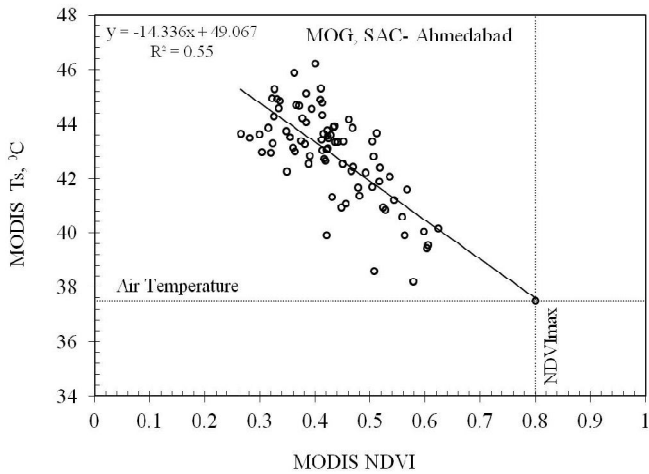
PAPER 2

Fig. 2: Example of Ts–NDVI correlation for a 9×9 pixel window around the MOG-SAC, Ahmedabad AWS field site. Ta$_{max}$ is estimated by extending the regression line to an NDVI for full vegetation cover
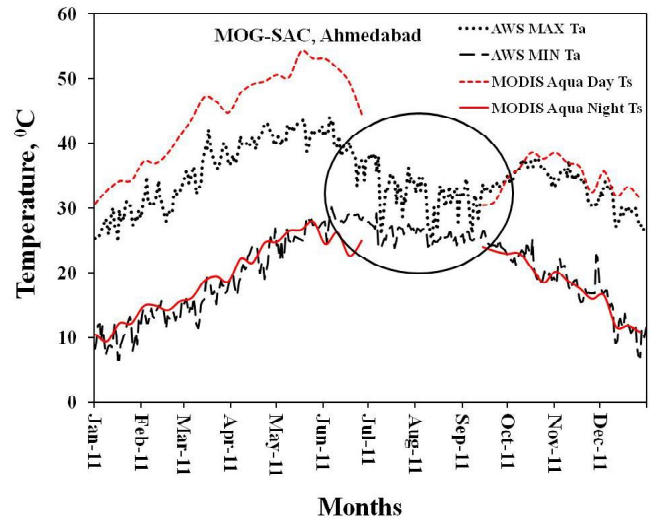

Fig. 3: Above graph depicts the minimum and maximum air temperature profile derived from AWS measurements and MODIS day and night Ts data for the year 2011. The data gap is due to the persistent cloud cover
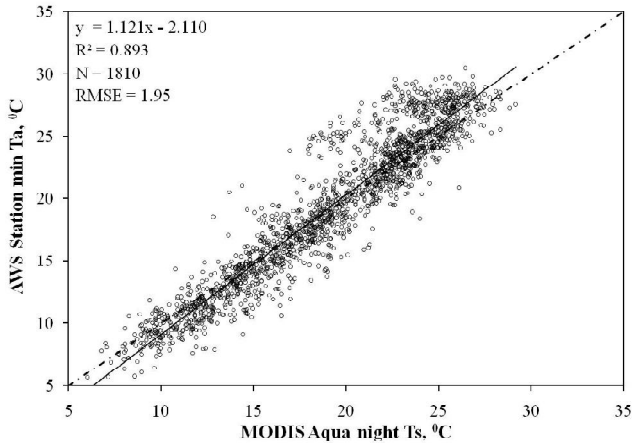

Fig. 4: Scatter plot between AWS minimum Ta and MODIS (Aqua) derived night Ts
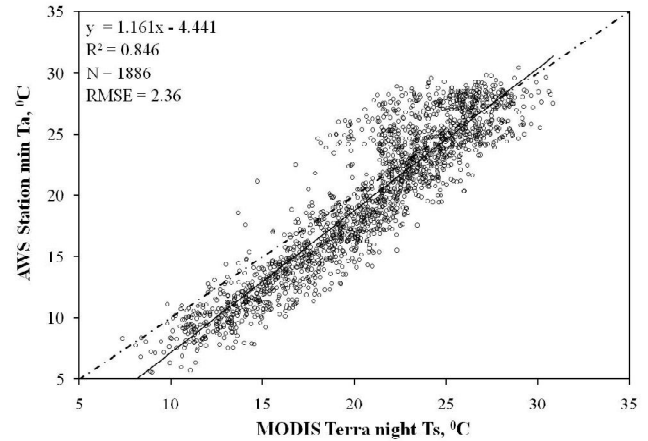

Fig. 5: Scatter plot between AWS-measured minimum Ta and MODIS (Terra) derived night Ts showing a good linear relationship

Fig. 6 Histogram showing the difference between minimum Ta estimated by the MODIS (Aqua) and minimum Ta measured by the 47 AWS ground stations of Gujarat for the year 2011

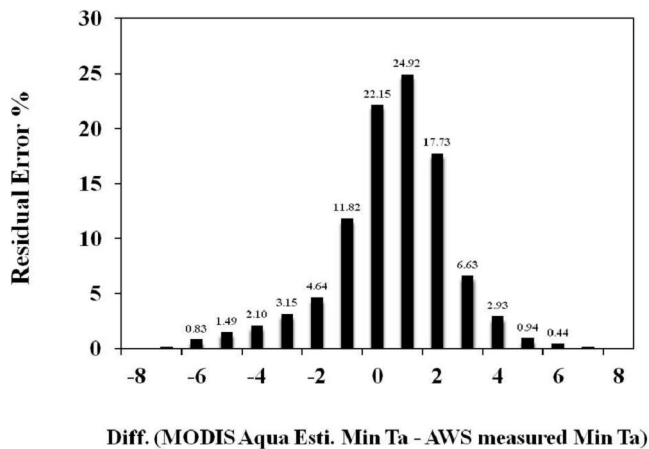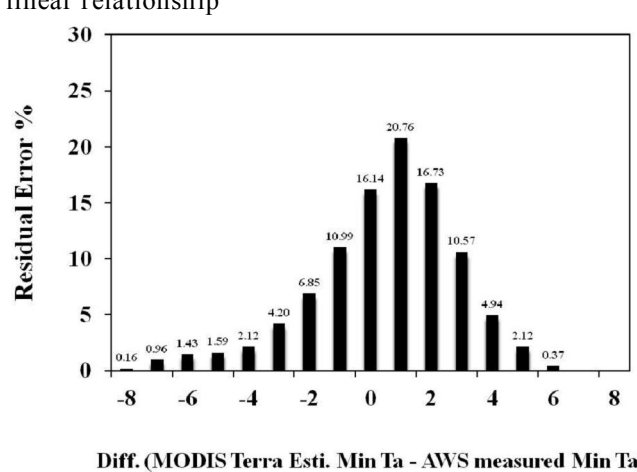**Fig. 7:** Histogram showing the difference between minimum Ta estimated by the MODIS (Terra) and minimum Ta measured by the 47 AWS ground stations of Gujarat for the year 2011
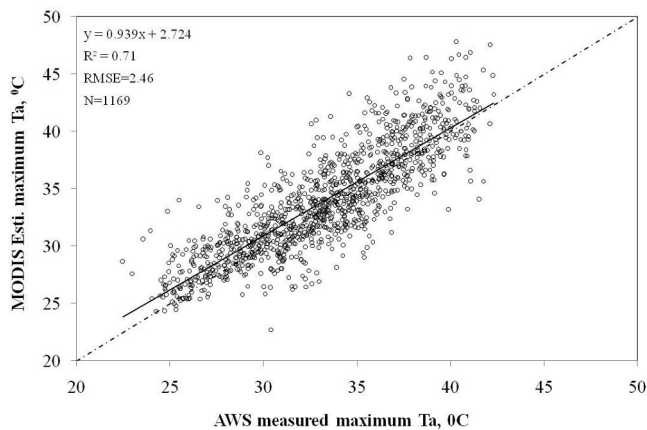
PAPER 2

Fig. 8: Comparison between MODIS (Aqua) derived maximum Ta and AWS-measured maximum Ta

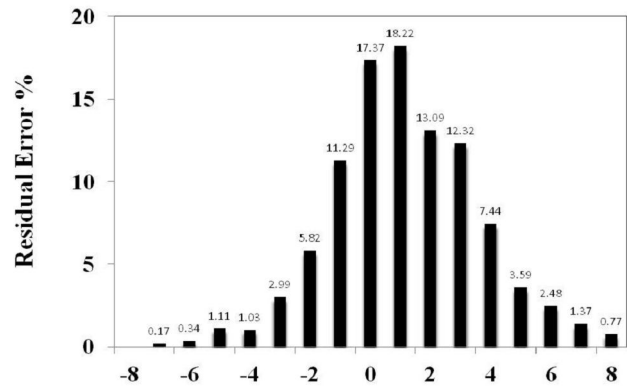**Diff. (MODIS Aqua Esti. Max Ta - AWS measured Max Ta)**

Fig. 9: Histogram showing the difference between maximum Ta retrieved by the MODIS (Aqua) and maximum Ta measured by the 47 AWS ground stations of Gujarat for the year 2011

Table 1: Monthly dependency of MAE, SD and MD for MODIS Aqua and Terra estimated minimum Ta with AWS minimum Ta. Months starting with prefix * indicates intense cloud occurrence.

Month	MODIS Aqua			MODIS Terra		
	MAE	SD	MD	MAE	SD	MD
January	1.29	1.68	0.03	1.54	1.88	0.51
February	1.18	1.51	0.38	1.44	1.65	0.74
March	1.29	1.61	0.62	2.00	1.88	1.51
April	1.20	1.60	-0.01	1.42	1.75	0.58
May	1.02	1.27	0.20	1.58	1.78	0.80
*June	2.85	1.73	-2.86	3.16	2.37	-2.67
*July	3.30	2.48	-3.72	3.28	2.99	-3.06
*August	3.41	2.33	-3.53	3.71	2.56	-3.42
September	1.60	2.19	0.21	2.00	2.04	-1.42
October	1.06	1.09	0.75	0.97	1.23	0.35
November	1.52	1.95	0.67	1.49	1.82	0.50
December	1.19	1.42	0.53	1.54	1.81	0.69
All Data	1.45	1.96	0.16	1.81	2.37	0.30

These data were downloaded from Level 1 and Atmosphere Archive and Distribution System (LAADS) Web data archive centre (http://ladsweb.nascom.nasa.gov). The spatial resolution of MODIS 8-day Ts data is 0.93 km. The equatorial passing time of MODIS-Terra is around 10:30 am/pm and of MODIS-Aqua is around 01:30 am/pm.

The MODIS 8-day composite Ts product was used to estimate minimum Ta. While, the MODIS 16-day composite NDVI product (MOD013A2) was used along with MODIS 8-day composite Ts product to estimate maximum Ta using TVX approach. In order to match the compositing period of NDVI with that of Ts for use in the TVX approach, the NDVI data was interpolated to 8-day composite from the two closest datasets.

Minimum Ta estimation

During the night, retrieval of Ta_{min} is simpler as the solar radiation does not affect the atmosphere as well as Earth's surface. So for Ta_{min} estimation, MODIS 8-day composite Ts observations were regressed with AWS Ta_{min} observations for 49 stations. In order to achieve this comparison, following procedure was carried out: (i) MODIS Ts data were extracted for a region of 3×3 pixels around the AWS stations, (ii) when a difference of more than seven degrees was found between two successive observations of Ta_{min} at any AWS, such observations were removed, (iii) Ta_{min} measurements of AWS were averaged every 8 days from the daily values for its comparison with MODIS 8-day Ts data, (iv) the linear regression analysis between night time MODIS Ts and AWS measured Ta_{min}, (v) analyzing the statistical difference between MODIS estimated and AWS measured Ta_{min}, and (vi) the accuracy for Ta_{min} was computed for both Aqua and Terra in order to evaluate the effect of the satellite overpass time.

Maximum Ta estimation

During daytime, a strong negative correlation is typically found between surface temperature and NDVI in

PAPER 2

Table 2: *Monthly MAE for maximum Ta predicted using different values of NDVI$_{max}$. Months starting with prefix * indicates intense cloud occurrence.*

Month	MAE for Different values of NDVI$_{max}$									
	1.00	**0.95**	**0.90**	**0.85**	**0.80**	**0.75**	**0.70**	**0.65**	**0.60**	**0.55**
January	1.76	**1.67**	1.90	2.21	2.60	3.04	3.49	3.94	4.38	4.83
February	2.35	**2.30**	2.35	2.53	2.83	3.24	3.72	4.23	4.78	5.33
March	3.75	3.43	3.20	**3.15**	3.29	3.61	4.09	4.68	5.35	6.09
April	5.34	4.83	4.39	4.01	3.77	**3.65**	3.66	3.84	4.19	4.78
May	5.16	4.64	4.17	3.86	3.66	**3.65**	3.85	4.31	4.91	5.67
*June	11.33	10.20	9.13	8.18	7.25	6.39	5.59	5.08	4.73	**4.46**
*July	8.90	8.48	8.06	7.64	7.22	6.80	6.38	5.96	5.54	**5.12**
*August	12.26	11.68	11.17	10.65	10.14	9.63	9.12	8.60	8.09	**7.58**
September	3.32	3.01	2.73	2.47	2.25	**2.10**	2.11	2.18	2.30	2.50
October	3.48	3.04	2.65	2.28	1.99	**1.72**	1.79	1.95	2.25	2.65
November	2.21	1.95	1.75	1.61	**1.57**	1.64	1.83	2.12	2.51	2.94
December	1.48	**1.43**	1.48	1.60	1.82	2.12	2.47	2.85	3.25	3.64

local spatial array of observation which is termed as Temperature Vegetation Index (TVX approach). This correlation is calculated for different species of vegetation and sensors (Goward *et al.*, 1985; Nemani and Running, 1989; Price, 1990). In this method Ts and NDVI data are collected with moving window therefore it is also called contextual window method (Wloczyk *et al.*, 2011).

Following this TVX method, a linear regression was carried out between Ts and NDVI for the pixels within the window to generate the slope (*a*) and intercept (*b*) from the equation (1).

$$T_s = a \times NDVI + b ----- (1)$$

After calculating the slope and intercept, Ta$_{max}$ was estimated by replacing the NDVI by NDVI$_{max}$ which represents maximum vegetation cover in above equation. This is shown in the following equation (2) (example is presented in Fig. 2 for MODIS Ts – NDVI correlation for 9 × 9 pixel window around an AWS station located at MOG-SAC, Ahmedabad).

$$T_s = a \times NDVI_{max} + b \approx T_a ----- (2)$$

In this method assumption is such that there is a variation in the NDVI values within the window to have good correlation between Ts and NDVI. Previous studies (Czajkowski *et al.,* 1997) reported that highly populated vegetation may have lesser correlation which indicates that slope is more negative for agricultural crops than for forest. For some cases where land is barren and no variation in NDVI or due to presence of cloud in Ts data leads to positive slope for contextual window, those pixels were removed from the analysis because that is not the theoretical consideration in TVX approach.

The appropriate value of NDVI$_{max}$ for study region along with the slope and intercept must be used to calculate the Ta$_{max}$ for that contextual window. Earlier studies based on field experiments, satellite data analysis and radiative transfer models have reported NDVI$_{max}$ values ranging from 0.65 to 0.90 (Price (1990); Goward (1997); Stisen *et al.* (2007); Nieto *et al.* (2010); Lakshmi *et al.* (2001); Boegh *et al.* (1999)). However, no values of NDVI$_{max}$ have been reported over Indian landmass. Therefore different values of NDVI$_{max}$ were tested for the study region to have the best estimation of Ta$_{max}$. In this method the window must have enough pixels (here 9 x 9 pixels window) to make a strong correlation excluding the pixels with negative NDVI (corresponding to water) or no data (corresponding to cloudy pixels).

RESULTS AND DISCUSSION

The Ta_{min} and Ta_{max} data derived from 47 AWS ground stations located in different parts of Gujarat were compared with day and night data of MODIS Ts extracted from 3×3 pixel window around the each AWS station. Fig. 3 shows an example of the temporal variations of Ta_{min} and Ta_{max} along with the MODIS Ts obtained for a station of MOG-SAC, Ahmedabad. Fig. 3 confirms that both Ts and Ta have seasonal cycles and their seasonal cycles are very much similar due to energy exchange between Ts and Ta depending on seasonal variation of incoming solar irradiance. The section marked with oval shape in Fig. 3 illustrates data gap in the MODIS products due to clouds. The other AWS observations also have similar kind of trends. During night time, good temporal agreement was observed between minimum Ta and Ts while significant difference was found during day time.

Estimation of minimum Ta using statistical analysis

In order to derive the Ta_{min}, a linear regression model was developed between AWS-measured minimum Ta and MODIS-derived Ts for all 47 stations. Scatter plot between MODIS Aqua night Ts and AWS minimum Ta for all the stations (Fig. 4) showed the coefficient of determination (R^2) was 0.90 with the RMSE of 2.16 ^0C. When the regression model was used to estimate the Ta_{min} from the MODIS Ts, a good accuracy was observed with median of 0.16, standard deviation (SD) of 1.96 and mean absolute error (MAE) of 1.45 ^0C for the night time MODIS-Aqua Ts observations. Accuracy was also estimated by calculating the residual error of MODIS Aqua estimated Ta_{min} and AWS measured Ta_{min} (Fig. 6). Using MODIS Aqua, 91% of estimated Ta_{min} residual error is within 3 ^0C of actual Ta_{min} and 99% of the estimated Ta_{min} is within 5 ^0C

Similar analysis was also carried out for the MODIS Terra night Ts to enumerate the dependency of time of overpass during the night time as Terra passes about 3 hour earlier than Aqua. We computed the same statistical variables for MODIS Terra night Ts and AWS minimum Ta. The coefficient of determination (R^2) between night time MODIS Terra Ts and AWS Ta_{min} was 0.85 and RMSE was 2.36 ^0C (Fig. 5). It was confirmed from this analysis that SD and MAE were also higher than for the Aqua data (1.96 vs. 2.37, 1.45 vs. 1.81). Residual error of MODIS Terra estimated Ta_{min} and AWS measured Ta_{min} (Fig. 7) showed that 86% of estimated Ta_{min} is within 3 ^0C of actual

Ta_{min} and 97% of the estimated Ta_{min} is within 5 ^0C. Hence, we found that MODIS Aqua Ts data is most accurate for estimating Ta_{min}. Further, annual variability presented in Table 1 showed that the lowest accuracy and highest bias are found during monsoon season i.e. from June to September. The bias can be cause by the influence of cirrus or near edge cloud present in MODIS Ts data.

Estimating maximum Ta using TVX approach

Regression equations for NDVI-Ts were calculated for 47 AWS measurements on 8-day composite MODIS Aqua data for the year 2011. Ta_{max} was estimated by extrapolating the NDVI-Ts regression line to a maximum value of $NDVI_{max}$ for effective full vegetation cover. In this study Ta_{max} was estimated using different values of $NDVI_{max}$ varied from 0.55 to 1 in increment of 0.05. This estimated Ta_{max} for all value of $NDVI_{max}$ was then compared with the Ta_{max} measured from the AWS ground network. MAE for each $NDVI_{max}$ values was calculated between MODIS derived Ta_{max} and AWS measured Ta_{max} as accentuated in Table 2. It shows that monthly dependency of $NDVI_{max}$ (number with bold) was performing well. The scatter plot between MODIS derived Ta_{max} and AWS measured Ta_{max} (Fig. 8) showed overall strong correlation (R^2) of 0.71. Accuracy was also estimated by calculating the residual error of MODIS estimated Ta_{max} and AWS measured Ta_{max} for different values of $NDVI_{max}$ (Fig. 9). It was shown that about 47 % of all measurement had deviation smaller than 1 ^0C, 66 % smaller than 2 ^0C, 81 % smaller than 3 ^0C, and only less than 6 % measurements had deviation larger than 5 ^0C. With the use of this approach, it was possible to estimate Ta_{max} with the MAE of 1.67 ^0C and RMSE of 2.46 ^0C. The results showed similar performances compared to previous studies by Czajkowski *et al.*, (1997) in Canada (RMSE = 4.2 ^0C), Prihodko and Goward (1997) in Kanas, (RMSE = 2.9 ^0C) and Prince *et al.*, (1998). This study shows how the idea of applying the TVX method as a moving window is appealing because it enables us to preserve the unique feature of the satellite data to estimate Ta_{max}. Table 2 showed that better accuracy was found during winter season (i.e. from November to February) and lowest accuracy was found during monsoon season because of cloud contamination in Ts and NDVI data (i.e. from June to September). Some of the synoptic sites might be located inappropriately regarding the TVX method where estimation of Ta_{max} is not possible, e.g. in build up or coastal areas. E.g. the stations PRL Ahmedabad and INS Dwarka-Okha might not be located within a pixel

window that fulfills the assumptions behind the TVX method. TVX performance is also dependent on topographic variability within the pixel and within the moving window, as it was expected. The higher variation in altitudes within the pixel and within the moving window increase the error in estimation of Ta$_{max}$ because it enhances the possibility of different atmospheric forcing, caused either by differences in solar radiation and wind speed, as well as the adiabatic cooling of air with altitude.

Sources of the uncertainty may come from the cloud and aerosol contaminated data points. The error in MODIS Ts contaminated by clouds and heavy aerosols can be very large (3–7 °C) (Wan and Li, 2008). The Ts values that are severely contaminated by clouds and heavy aerosols were removed from Collection-5 Level-3 MODIS Ts products using empirical constraints on temporal variations in clear-sky Ts. However, it is very difficult for the MODIS cloud-mask to discriminate all pixels affected by clouds and heavy aerosols from clear sky pixels, particularly near cloud edges, cirrus and/or with sub-pixel clouds.

CONCLUSION

This study presented different approaches for estimating Ta$_{min}$ and Ta$_{max}$ from the satellite platform using the MODIS data along with the AWS measurements over 47 stations located in different parts of Gujarat. The Ta$_{min}$ was successfully retrieved through a regression analysis between night time MODIS Ts and AWS measured minimum Ta over all stations. The uncertainty of the estimated Ta$_{min}$ is about 1.45 ^{0}C (MAE) and 2.16 ^{0}C (RMSE), which implies good performance of the method. Besides this, the effect of the time of overpass was also analyzed by comparing Aqua and Terra estimations and it was confirmed that Aqua provides the most accurate estimation. The Ta$_{max}$ was retrieved using a TVX approach with an accuracy of about 1.67 ^{0}C (MAE) and 2.46 ^{0}C (RMSE). This result indicates the physical power of the approach and supports the application of the produced data set in a modeling framework.

REFERENCES

Boegh, E., Soegaard, H., Hanan, N., Kabat, P., and Lesch, L. (1999). A remote sensing study of the NDVT-Ts relationship and the transpiration from sparse vegetation in the Sahel based on high-resolution satellite data. *Remote Sens. Environ.*, 69: 224-240.

Cresswell, M. P., Morse, A. P., Thomson, M. C., and Connor, S. J. (1999). Estimating surface air temperatures, from Meteosat land surface temperatures, using an empirical solar zenith angle model. *Int. J. Remote Sens.*, 20(6): 1125-1132.

Czajkowski, K. P., Mulhern, T., Goward, S. N., Cihlar, J., Dubayah, R.O., and Prince, S. D. (1997). Biospheric environmental monitoring at BOREAS with AVHRR observations. *J. Geophy. Res., [Atmospheres]*, 102(29): 651-662.

Davis, F.A., and Tarpley, J.D., (1983). Estimation of shelter temperatures from operational satellite sounder data. *J. Applied Meteorol.,* 22(3): 369-376.

Florio E. N., Lele, S. R., Chang, Y. C., Sterner R. and Glass G. E. (2004): Integrating AVHRR satellite data and NOAA ground observations to predict surface air temperature: a statistical approach , *Int. J. Remote Sens.*, 25(15): 2979-2994

Goward, S. N., Cruickshanks, G. D., and Hope, A. S. (1985). Observed relation between thermal emission and reflected spectral radiance of a complex vegetated landscape. *Remote Sens. Environ.*, 18: 137-146.

Goward, S. N., Waring, R. H., Dye, D. G., and Yang, J. L. (1994). Ecological remote-sensing at OTTER- Satellite macroscale observations. *Ecological Applications*, 4: 322-343.

Greena, R.M., and Hay, S.I., (2002). The potential of Pathfinder AVHRR data for providing surrogate climatic variables across Africa and Europe for epidemiological applications. *Remote Sens. Environ.,* 79: 166-175.

Jang, J. D., Viau, A. A., and Anctil, F. (2004). Neural network estimation of air temperatures from AVHRR data. *Int. J. Remote Sens.*, 25: 4541-4554.

Lakshmi, V., Czajkowski, K., Dubayah, R., and Susskind, J. (2001). Land surface air temperature mapping using TOVS and AVHRR. *Int. J. Remote Sens.*, 22: 643-662.

Nemani, R. R., and Running, J. W. (1989). Estimation of regional surface resistance to evapotranspiration from NDVI and thermal-IR AVHRR data. *J. Applied Meteorol.*, 28: 276"284.

Nieto, H., Aguado, I., Chuvieco, E., and Sandholt, I. (2010). Dead fuel moisture estimation with MSG-SEVIRI

data. Retrieval of meteorological data for the calculation of the equilibrium moisture content. *Agri. Forest Meteorol.*, 150: 861-870.

Oke, T. R. (1987). *"Boundary Layer Climates"*, 2nd edn, Routledge, London, 435 pp.

Price, J. C. (1990). Using spatial context in satellite data to infer regional scale evapotranspiration. *IEEE Trans Geosci. Remote Sens.*, 28, 940-948.

Prihodko, L. and Goward, S.N., (1997). Estimation of air temperature from remotely sensed surface observations. *Remote Sens. Environ.*, 60: 335-346.

Prince, S. D., Goetz, S. J., Dubayah, R. O., Czajkowski, K. P., and Thawley, M. (1998). Inference of surface and air temperature, atmospheric precipitable water and vapor pressure deficit using Advanced Very High-Resolution Radiometer satellite observations: Comparison with field observations. *J. Hydrol.*, 213: 230-249.

Stisen, S., Sandholt, I., Norgaard, A., Fensholt, R., and Eklundh, L. (2007). Estimation of diurnal air temperature using MSG SEVIRI data in West Africa. *Remote Sens. Environ.*, 110(2): 262-274.

Sun, Y. J., Wang, J. F., Zhang, R. H., Gillies, R. R., Xue, Y., and Bo, Y. C. (2005). Air temperature retrieval from remote sensing data based on thermodynamics. *Theor. Applied Climatol.*, 80(1): 37-48.

Vancutsem, C., Ceccato, P., Dinku, T., and Connor, S. J. (2010). Evaluation of MODIS land surface temperature data to estimate air temperature in different ecosystems over Africa. *Remote Sens. Environ.*, 114(2): 449-465.

Vogt, J. V., Viau, A. A., and Paquet, F. (1997). Mapping regional air temperature fields using satellite-derived surface skin temperatures. *Intern. J. Climatol*, 17: 1559"1579.

Willmott, C. J., Robeson, S. M., and Feddema, J. J. (1991). Influence of spatially-variable instrument networks on climatic averages. *Geophy. Res. Letters*, 18: 2249-2251.

Wan, Z., and Dozier, J., (1996). A generalised split-window algorithm for retrieving land surface temperature from space. *IEEE Trans. Geosci. and Remote Sens.* 34 (4): 892-905.

Wan, Z., and Li, Z. L., (2008). Radiance-based validation of the V5 MODIS land-surface temperature product. *Int. J. Remote Sens.,* 29: 5373-95

Wloczyk, C., Borg, E., Richter, R., and Miegel, K., (2011): Estimation of instantaneous air temperature above vegetation and soil surfaces from Landsat 7 ETM+ data in northern Germany, *Int. J. Remote Sens.*, 32(24): 9119-9136

Zaksek, K., and Schroedter-Homscheidt, M., (2009). Parameterization of air temperature in high temporal and spatial resolution from a combination of the SEVIRI and MODIS instruments. *ISPRS J. Photogram. Remote Sens.*, 64(4): 414-421.

PAPER 2